# Polarization and energy dynamics in ultrafocused optical Kerr propagation

**A. Ciattoni**

*Dipartimento di Fisica, Università Roma Tre, I-00146 Rome, Italy, and Istituto Nazionale di Fisica della Materia, Unità di Roma 3, Rome, Italy*

**C. Conti**

*Istituto Nazionale di Fisica della Materia, Unità di Roma 3, Rome, Italy*

**E. DelRe and P. Di Porto**

*Dipartimento di Fisica, Università dell'Aquila, 67100 Aquila, Italy, and Istituto Nazionale di Fisica della Materia, Unità di Roma "La Sapienza," 00185 Rome, Italy*

**B. Crosignani and A. Yariv**

*Department of Applied Physics, California Institute of Technology, Pasadena, California 91125*

Received October 22, 2001

Developing a complete vectorial description of optical nonparaxial propagation of highly focused beams in Kerr media, we disclose a family of new phenomena. These phenomena appear to emerge as a consequence of the mutual coupling of all three components of the optical field. This circumstance, which is intrinsic to the very nature of Kerr propagation, was previously discarded on the basis of the conjecture that a reduced system is possible in which only one transverse field component interacts with the longitudinal component. 

*OCIS codes:* 190.3270, 260.5950.

Optical beams focused down to spatial scales of the order of the carrier wavelength undergo nontrivial dynamics that are associated mainly with nonparaxial effects. In nonlinear media this regime can become dominant even with initially quasi-planar (paraxial) beams. This is the case with the paradigm Kerr nonlinearity, where self-focusing naturally violates paraxial conditions and brings the system into the still not well understood realm of nonparaxial nonlinear propagation. Several initial studies based on a variety of different scalar approaches resulted in a first important prediction: The catastrophic beam collapse associated with the nonlinear Schrödinger model is bleached by nonparaxiality.[1–5] More-sophisticated approaches[6–11] recently showed how vectorial effects, neglected in previous studies, play a fundamental role in determining beam evolution. These approaches hinge on a partial vectorial correction, taking into account the role played by the longitudinal field component, allowing a deeper understanding of beam evolution. For example, beam filamentation,[12] previously thought to be associated with spontaneous noise amplification, has been attributed to deterministic symmetry breaking.

In general, our understanding of these effects is burdened both by the complexity of the associated nonlinear model and by the limited availability of experimental results. In this Letter we illustrate a new theoretical, fully vectorial approach to nonparaxial Kerr propagation, based on a perturbative treatment that does not require any *a priori* simplifying reduction to a two-component vector system. Our results indicate a series of qualitatively new phenomena that stem from mutual energy exchange of the two transverse vector components, which have been structurally excluded by previous theories.

In a recent paper[13] we derived an appropriate set of equations that describe propagation of a monochromatic field in the presence of a real anisotropic refractive-index perturbation $\overleftrightarrow{\delta \mathbf{n}}$ relative to a homogeneous background and that contains all-order nonparaxial corrections in the smallness parameter, $\epsilon = \lambda/(n_0 r_0)$, where $\lambda$ is the wavelength *in vacuo*, $n_0$ is the linear refractive index, and $r_0$ is the transverse beam scale (waist). This derivation, starting directly from Maxwell's equations with no approximations and without neglecting any vectorial contribution, is exact to all orders in $\epsilon$.

To tackle Kerr propagation characterized by a complex Hermitian $\overleftrightarrow{\delta \mathbf{n}}$, we formulate the appropriate equation that describes the evolution of the forward-traveling transverse part, $\mathbf{A}_\perp(\mathbf{r}_\perp, z) = \exp(ikz) \times \mathbf{E}_\perp(\mathbf{r}_\perp, z)$, of the field, where $k = \omega n_0/c$ and $\mathbf{r}_\perp = x\hat{\mathbf{x}} + y\hat{\mathbf{y}}$. Considering only terms up to the second order in $\epsilon$, we are able to predict and describe all relevant phenomena associated with nonparaxial effects. For a dielectric-constant distribution of the type $\overleftrightarrow{\epsilon} = {n_0}^2 \overleftrightarrow{\mathbf{I}} + 2n_0 \overleftrightarrow{\delta \mathbf{n}}$, where $\overleftrightarrow{\delta \mathbf{n}}$ is a $3 \times 3$ Hermitian tensor representing the refractive-index perturbation and $\{\overleftrightarrow{\mathbf{I}}\}_{ij} = \delta_{ij}$, the propagation equation reads as

$$\left[ i \frac{\partial}{\partial z} + \frac{1}{2k} {\nabla_\perp}^2 - \frac{1}{8k^3} ({\nabla_\perp}^2)^2 \right] \mathbf{A}_\perp = -\frac{k}{n_0} \overleftrightarrow{\delta \mathbf{n}}_\perp \mathbf{A}_\perp - \frac{i}{n_0} \delta \mathbf{n}' (\nabla_\perp \cdot \mathbf{A}_\perp) - \frac{i}{n_0} \nabla_\perp (\delta \mathbf{n}'^* \cdot \mathbf{A}_\perp) + \frac{1}{2n_0 k} {\nabla_\perp}^2 (\overleftrightarrow{\delta \mathbf{n}}_\perp \mathbf{A}_\perp) + \frac{1}{n_0} \nabla_\perp [\delta n_{zz} (\nabla_\perp \cdot \mathbf{A}_\perp)] - \frac{1}{n_0 k} \nabla_\perp [\nabla_\perp \cdot (\overleftrightarrow{\delta \mathbf{n}}_\perp \mathbf{A}_\perp)], \quad (1)$$

 

where $\nabla_\perp = \hat{\mathbf{x}}\partial_x + \hat{\mathbf{y}}\partial_y$, $\delta\mathbf{n}' = \delta n_{xz}\hat{\mathbf{x}} + \delta n_{yz}\hat{\mathbf{y}}$, and $\overleftrightarrow{\delta\mathbf{n}}_\perp$ is the $2 \times 2$ tensor obtained from $\overleftrightarrow{\delta\mathbf{n}}$ by suppression of the third row and column, and the standard row-by-column product is implicit in multiplying tensors and vectors. Once Eq. (1) is solved for $\mathbf{A}_\perp$, the longitudinal component $A_z$ can be derived from it, to first order in $\epsilon$, by means of the relation [see Eq. (F7) of Ref. 13]

$$A_z = \frac{i}{k}\nabla_\perp \cdot \mathbf{A}_\perp\,. \tag{2}$$

We emphasize that Eq. (1) differs from Eq. (31) derived in Ref. 13 in that Eq. (1) allows $\{\overleftrightarrow{\delta\mathbf{n}}\}_{ij}$ to be complex. For a Kerr medium,

$$\overleftrightarrow{\delta\mathbf{n}}_\perp = \frac{2}{3}n_2\begin{bmatrix} |\mathbf{A}|^2 + \frac{1}{2}|A_x|^2 & \frac{1}{2}A_yA_x{}^* \\ \frac{1}{2}A_xA_y{}^* & |\mathbf{A}|^2 + \frac{1}{2}|A_y|^2 \end{bmatrix}, \tag{3}$$

$$\delta\mathbf{n}' = \frac{1}{3}n_2A_z\mathbf{A}_\perp{}^*, \tag{4}$$

$$\delta n_{zz} = \frac{2}{3}n_2|\mathbf{A}_\perp|^2 + n_2|A_z|^2, \tag{5}$$

where $n_2$ is the so-called nonlinear refractive-index coefficient.[14] Inserting Eqs. (3)–(5) into Eq. (1) and using Eq. (2), we obtain

$$\begin{aligned}\left[i\frac{\partial}{\partial z} + \frac{1}{2k}\nabla_\perp{}^2 - \frac{1}{8k^3}(\nabla_\perp{}^2)^2\right]\mathbf{A}_\perp &= -\frac{2k}{3}\frac{n_2}{n_0}|\mathbf{A}_\perp|^2\mathbf{A}_\perp \\ &- \frac{k}{3}\frac{n_2}{n_0}(\mathbf{A}_\perp\cdot\mathbf{A}_\perp)\mathbf{A}_\perp{}^* - \frac{2}{3k}\frac{n_2}{n_0}|\nabla_\perp\cdot\mathbf{A}_\perp|^2\mathbf{A}_\perp \\ &- \frac{1}{3k}\frac{n_2}{n_0}\nabla_\perp[(\mathbf{A}_\perp\cdot\mathbf{A}_\perp)(\nabla_\perp\cdot\mathbf{A}_\perp{}^*)] \\ &+ \frac{1}{3k}\frac{n_2}{n_0}(\nabla_\perp\cdot\mathbf{A}_\perp)^2\mathbf{A}_\perp{}^* + \frac{1}{3k}\frac{n_2}{n_0}\nabla_\perp{}^2(|\mathbf{A}_\perp|^2\mathbf{A}_\perp) \\ &+ \frac{1}{6k}\frac{n_2}{n_0}\nabla_\perp{}^2[(\mathbf{A}_\perp\cdot\mathbf{A}_\perp)\mathbf{A}_\perp{}^*] \\ &+ \frac{2}{3k}\frac{n_2}{n_0}\nabla_\perp[(\nabla_\perp\cdot\mathbf{A}_\perp)|\mathbf{A}_\perp|^2] \\ &- \frac{2}{3k}\frac{n_2}{n_0}\nabla_\perp[\nabla_\perp\cdot(|\mathbf{A}_\perp|^2\mathbf{A}_\perp)] \\ &- \frac{1}{3k}\frac{n_2}{n_0}\nabla_\perp\{\nabla_\perp\cdot[(\mathbf{A}_\perp\cdot\mathbf{A}_\perp)\mathbf{A}_\perp{}^*]\},\end{aligned} \tag{6}$$

which describes nonparaxial Kerr nonlinear propagation.

Equation (6) is fully vectorial and does not admit of linearly polarized solutions. In fact, even if the $y$ component $A_y$ is assumed to be zero at $z = 0$, it will not remain so, because of the presence of terms containing $A_x$ alone in the right-hand side of the $y$ component of Eq. (6). Clearly, this mathematical property does not always require that one use a fully vectorial treatment to acquire a more comprehensive understanding of propagation. In fact, previous theoretical predictions are based on the conjecture that mutual coupling between $A_x$ and $A_y$ gives negligible effects. The preliminary results below, however, show that, in the highly nonparaxial regime, following self-focusing, full vectorial coupling is one of the fundamental mechanisms driving beam evolution.

We carried out numerical simulations based on Eq. (6) in its appropriate normalized form. Given the characteristics of our model, we employed a standard split-step fast Fourier transform method and analyzed the dynamics for an input Gaussian, linearly $x$-polarized beam. The beam's spot size, $r_0$, fixes the value of the perturbative parameter, $\epsilon$. We have thus investigated beam self-focusing dynamics (Figs. 1 and 2).

When the input peak power exceeds the critical value, $P_c$, prescribed by standard paraxial theory, ultrafocusing takes place. In this ultrafocused (nonparaxial) regime, $A_x$ becomes an efficient source for the orthogonal transverse component, $A_y$. As a result the polarization acquires a structure. Considering the evolution of the Poynting vector, $\mathbf{S}$ (Fig. 1), we find that (at the considered order in $\epsilon$) the longitudinal component, $S_z$, remains the same as that predicted by paraxial theory. However, in the nonparaxial regime $S_x$ and $S_y$ come into play and give rise to lateral dipolelike emission. More precisely, we note that, whereas during self-focusing ($z < 4Z_d$, where $Z_d = kr_0{}^2$ is the diffraction length) the (weak) transverse components of $\mathbf{S}$ are directed

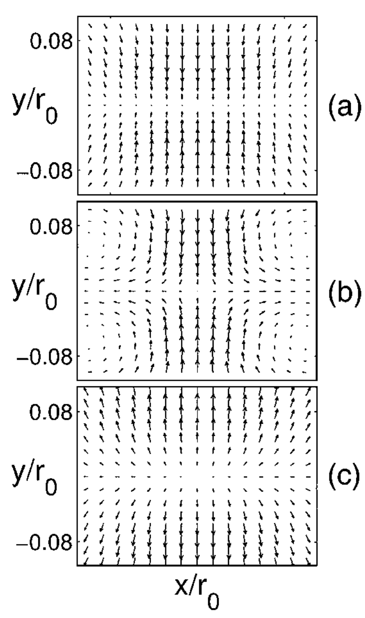


Fig. 1. Transverse Poynting vector $\mathbf{S}_\perp$ distribution during collapse according to Eq. (1). (a) Self-focusing up to $z = 4Z_d$. (b) Anisotropic structures at $z = 4.18Z_d$. (c) Onset of ultradiffraction at $z = 4.24Z_d$.

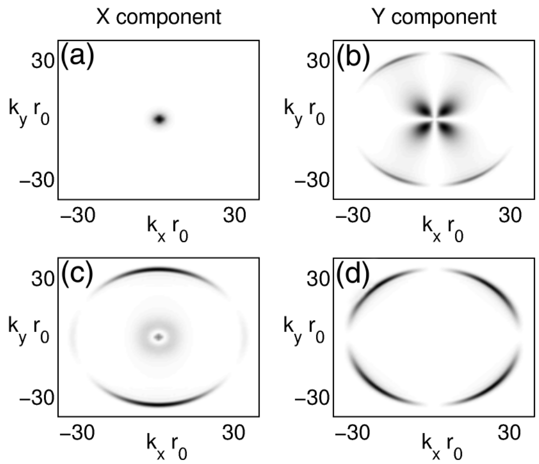


Fig. 2. Spatial spectra (a), (c) $A_x$ and (b), (d) $A_y$, according to Eq. (1) for (a), (b) $z = 4.04Z_d$ and (c), (d) $z = 4.20Z_d$. Note the remarkable parametriclike excitation of strongly tilted modes.

toward the center of the beam [see Fig. 1(a)], in the ultrafocused condition ($z > 4Z_d$) the vector field, $\mathbf{S}_\perp$, evolves into a saddlelike pattern characterized by $x$-directed emission and $y$-directed compression [Fig. 1(b)]. This highly anisotropic configuration is enforced by coupling back of energy from $A_y$ to $A_x$. Clearly this mutual energy exchange between $A_x$ and $A_y$ is the mechanism leading to the breaking of the circular symmetry of the beam.

The simulation is carried out for the case of $\lambda/(n_0 r_0) = 2\pi 0.06 \cong 0.38$ (corresponding to $\sigma = 0.06$ in the notation of Ref. 10), with input peak power $P = 1.9P_r$ [with $P_r = c\epsilon_0 \lambda^2/(8\pi^2 n_2 {r_0}^2)$] very close to the critical power for the collapse,[10] which appears, according to our simulations, in the proximity of $z = 4Z_d$.

Inspecting the spectral components of $A_{x,y}$ (Fig. 2) in the ultrafocusing regime, we see that the orthogonal (to the initial) polarization develops a ringlike structure denoting lateral emission [Fig. 2(b)]. The large angle of the corresponding anisotropic cone is indeed remarkable. Further propagation along $z$ also gives rise to a transfer (and rotation) of this structure to the $A_x$ component [Figs. 2(c) and 2(d)]. Nonlinear coupling between spectral components appears to have a parametric origin; it is maximum for a given angle and has a specific threshold.

Furthermore, our simulations indicate that the ultrafocusing regime is superseded by an ultradiffracting regime [Fig. 1(c)], and no periodic features in $z$ emerge. In contrast with the paraxial approximation, where $\mathbf{S}_\perp$ is totally neglected even in its realm of validity, our results describe its role both at the onset and during ultrafocused propagation.

Formally, Eq. (6) can be compared with the existing versions of the propagation equation only if we set $A_y = 0$, which amounts to assuming that $A_y$ remains negligible over the whole propagation distance. In this case our expression reduces to

$$\begin{aligned}\left[ i\frac{\partial}{\partial z} + \frac{1}{2k}{\nabla_\perp}^2 - \frac{1}{8k^3}({\nabla_\perp}^2)^2 \right] A_x = &-\frac{kn_2}{n_0}|A_x|^2 A_x \\ &+ \frac{1}{2k}\frac{n_2}{n_0}\frac{\partial^2}{\partial y^2}(|A_x|^2 A_x) - \frac{1}{3k}\frac{n_2}{n_0}A_x\frac{\partial^2 |A_x|^2}{\partial x^2} \\ &- \frac{1}{2k}\frac{n_2}{n_0}{A_x}^2\frac{\partial^2 {A_x}^*}{\partial x^2} - \frac{2}{k}\frac{n_2}{n_0}A_x\left|\frac{\partial A_x}{\partial x}\right|^2, \end{aligned} \tag{7}$$

which coincides with the one worked out in Ref. 10 by means of a different approach. This is not the case for other versions of the propagation equation, which do not coincide either with our expression or among themselves. For the addressable case of Ref. 10, the simulation described above gives completely different results, starting from the very same boundary conditions.

In conclusion, we believe that Eq. (6) represents, up to terms of second order in the smallness parameter $\epsilon = \lambda/(n_0 r_0)$, the correct version of the nonparaxial vectorial equation describing optical propagation in Kerr media. Numerical simulations indicate that a new family of propagation effects emerges in which full vectorial coupling of the transverse components plays a central role, in contrast with previous predictions.

This research was funded in part by the Istituto Nazionale Fisica della Materia through the "Soliton-based electro-optic structures in near-transition photorefractive crystals and bulk optical manipulation" project. The work at the California Institute of Technology was supported by the U.S. Office of Naval Research and the U.S. Air Force Office of Scientific Research. E. DelRe's e-mail address is eugenio.delre@aquila.infn.it.

## References

1. M. D. Fleit and J. A. Fleck, Jr., J. Opt. Soc. Am. B **5,** 633 (1988).
2. J. T. Manassah and B. Gross, Opt. Lett. **17,** 976 (1992).
3. N. Akhmediev, A. Ankiewicz, and J. M. Soto-Crespo, Opt. Lett. **18,** 411 (1993).
4. G. Fibich and G. C. Papanicolaou, Opt. Lett. **22,** 1379 (1997).
5. A. P. Sheppard and M. Haelterman, Opt. Lett. **23,** 1820 (1998).
6. S. Chi and Q. Cuo, Opt. Lett. **20,** 1598 (1995).
7. B. Crosignani, P. Di Porto, and A. Yariv, Opt. Lett. **22,** 778 (1997).
8. E. Granot, S. Sternklar, Y. Isbi, B. Malomed, and A. Lewis, Opt. Lett. **22,** 1290 (1997).
9. S. Blair and K. Wagner, Opt. Quantum Electron. **30,** 697 (1998).
10. R. De la Fuente, O. Varela, and H. Michinel, Opt. Commun. **173,** 403 (2000).
11. S. Blair, Chaos **10,** 570 (2000).
12. G. Fibich and B. Ilan, Opt. Lett. **26,** 840 (2001).
13. A. Ciattoni, P. Di Porto, B. Crosignani, and A. Yariv, J. Opt. Soc. Am. B **17,** 809 (2000).
14. B. Crosignani, A. Cutolo, and P. Di Porto, J. Opt. Soc. Am. **72,** 1136 (1982).